Geoderma 410 (2022) 115661

Contents lists available at ScienceDirect

Geoderma

journal homepage: www.elsevier.com/locate/geoderma

Statistical understanding for snow cover effects on near-surface ground temperature at the margin of maritime Antarctica, King George Island

Hyoun Soo Lim [a], Hyun-Cheol Kim [b], Ok-Sun Kim [b], Hyejung Jung [c], Jeonghoon Lee [c,*], Soon Gyu Hong [b]

[a] Dept. of Geological Sciences, Pusan National University, Busan 46231, Korea
[b] Korea Polar Research Institute, Incheon 21990, Korea
[c] Dept. of Science Education, Ewha Womans University, Seoul 03760, Korea

ARTICLE INFO

Handling Editor: Budiman Minasny

Keywords:
Ground surface temperature
Principal component analysis
Snow cover
King George Island

ABSTRACT

Snow cover plays an important role in water supply through melting of snow/ice in polar ecosystem and environments, in particular, Antarctica. Although a site access to Antarctica is high-priced, measurements of ground surface temperature (GST) using small self-recording temperature sensors (iButtons) can provide a powerful and relatively inexpensive approach to trace the spatial and temporal distributions of soil temperature and in addition, absence/presence of snow cover. In this study, principal component analysis (PCA) was utilized to explain major patterns of GST from 128 sites at King George Island in maritime Antarctica. Variations of GST were monitored between December 2011 and January 2013. The iButtons were initially installed in snow free areas in the austral summer of 2011. Principal components 1 and 2 were associated with air temperature and snow cover, respectively. Both PCs showed good correlations with the mean GST of JJA (June to August), not with that of DJF (December to January). Based on the results excluding an outlier, PCA divided the 127 GST observations into three groups effectively: absence of snow cover (Group 1), intermittent snow cover (Group 2), and presence of snow cover (Group 3). Snow cover can supply water to the ecosystem and the GST pattern of Group 2 may imply an abundance and high productivity of mosses in the study area. Using approaches suggested by previous studies, snow cover showed up nine days (days 317–326), and the melt-out date was day 326 (KG125 in Group 2). The GST data and statistical approaches used in this study can be useful in other GST studies, particularly, for both polar regions.

1. Introduction

Ground surface temperature (GST) is an essential indicator for hydrological, biological, and climatic processes since it can be a proxy for climatic components just above the ground surface, such as air temperature, snow cover and absorbed incoming shortwave radiation at the ground surface (Beltrami, 1996; Zhang, 2005; Vieira et al., 2017; Obu et al., 2020). In addition, it can be linked with ground surface characteristics, such as soil water distribution, species of vegetation and surface microrelief (Guglielmin, 2006; Hrbacek et al., 2020). GST is significantly influenced by land-surface and soil properties, vegetation, latent heat sources and sinks and permafrost distribution (Guglielmin et al., 2012; Oliva et al., 2017). Long-term observations of GST can be necessary to confirm and/or validate the global circulation models (GCMs), which have been used to predict future climate. Given the temporal variations of GST in both polar regions, especially in permafrost and periglacial environments, it is often most suitable to obtain continuous measurements of spatially distributed GST. Observations of GST can be a routine part of various types of study on soil science, polar science and ecology in the temperate and polar areas. On the ground, for instance, GST measurements are feasible by means of miniature temperature loggers, hand tests, or as part of more comprehensive measurement stations over the past decade (Lundquist and Lott, 2008).

The presence/absence of an insulating snow cover has an important effect on the ground thermal regime in both polar regions during the cold period of the annual temperature cycle (Zhang, 2005; Luo et al., 2019). Snow cover can reduce the loss of heat flow from the ground due to its low thermal conductivity (Staub and Delaloye, 2017). On the contrary, snow cover, which has the high albedo, limits heat flux from the atmosphere to the ground surface throughout the melting period

* Corresponding author.
E-mail address: jeonghoon.d.lee@gmail.com (J. Lee).

https://doi.org/10.1016/j.geoderma.2021.115661
Received 26 May 2021; Received in revised form 9 December 2021; Accepted 10 December 2021
Available online 16 December 2021

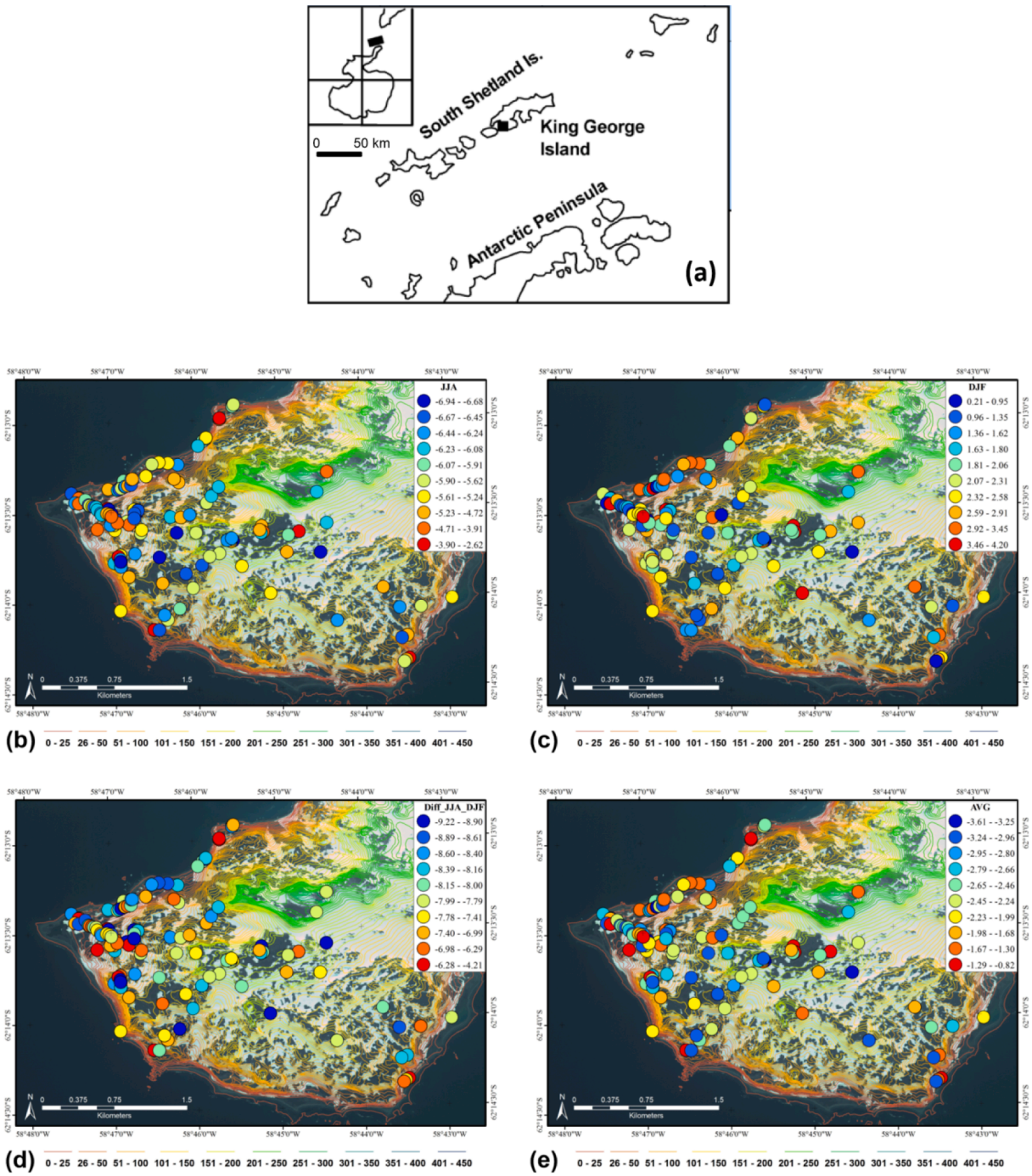

Fig. 1. Seasonal variations of ground surface temperature (GST) in the Barton Peninsula, Antarctica. The photo was taken by the KOMPSAT-2 (KOrea Multi-Purpose Satellite) on 16 January 2013. (a) Location of the study area, (b) mean values of JJA GST, (c) mean values of DJF GST, (d) mean values of GST for difference of two seasons, and (e) mean values of GST.

(Zhang, 2005). High latent heat due to snowmelt is a heat sink. Relying on the net heat balance from the ground and atmosphere and the amount of precipitation, permafrost may develop or be conserved at the bottom of both thin and thick snow cover (Zhao et al., 2018). The general effect of snow cover on the ground thermal region depends on the timing, duration and accumulation and melting processes of snow cover, as well as the interactions between snow cover and the micro-meteorological conditions, geographical location, local microrelief and vegetation (Zhang, 2005). In regions with continuous permafrost, snow cover can result in an increase of the mean annual ground and permafrost surface temperature by several degrees, whereas in regions with discontinuous and sporadic permafrost, the absence of seasonal snow cover may be a key feature for permafrost development (Zhang, 2005). Moreover, in regions with seasonally frozen ground, snow cover can considerably lower the seasonal freezing depth (Teubner et al., 2015).

GST provides not only an indicator of soil surface temperature and ground freezing state but also spatial representations of the presence or absence of snow cover when distributed (Schmid et al., 2012; Pedersen et al., 2018). It has been shown that GST data can serve as a proxy for presence/absence of snow cover due to the insulating effect of snow itself (Gądek and Leszkiewicz, 2010; Bender et al., 2020). When snow is present, soil does not experience strong diel fluctuations of air

temperature, whereas snow-free conditions are associated with larger daily fluctuation of GST. The reduction in the difference between the daily maximum and minimum GST in the presence of snow implies that the GST can be a suitable indicator for spatial distribution of snow cover. This is, in particular, valid during the snow-covered season, when the insulating properties of the snow cover provide stable thermal conditions in the sub-snow environment, including the vegetation cover and soil (Cannone and Guglielmin, 2009). In turn, the nutrient availability along with the meltwater released from the snow in spring regulates the vegetation growth far into the growing season (Kennedy, 1993). Thus, the snow condition in the preceding winter may have legacy influences on the following growing seasons, which makes snow observations essential for the understanding of ecosystem functions and feedbacks (Cannone and Guglielmin, 2009; de Pablo et al., 2017; Convey and Peck, 2019). This is also can be very helpful in many areas where remotely sensed data or direct observations are not available.

This work is a part of comprehensive understanding of interactions between the hydrosphere and biosphere in maritime Antarctic regions. Here, we present data from the Barton Peninsula, King George Island, to demonstrate how GST can be used to estimate the spatial distribution of snow cover measuring temporal variations of the GST. Since the terrestrial snow cover is a key variable controlling Antarctic ecosystem processes, the snow cover inferred from the observations of GST is valuable for explaining changes in both biotic and abiotic components of Antarctic ecosystems through hydrological processes (Hrbácek et al., 2020). In this study, we collected single-point measurements of time-series of GST at 128 sites in the Barton Peninsula over one year. The effectiveness of this work was evaluated using a multivariate statistical procedure, namely principal component analysis (PCA), to determine the major factors affecting the GST (Winter et al., 2000). PCA has previously been utilized to extract information on the dominating influences or processes and patterns from large environmental datasets (Lee et al., 2008; Nyamgerel et al., 2020). In this work, we use near-surface ground temperature measured at a depth of a few centimeters as a proxy for GST. We investigate the potential for GST to offer reliable, inexpensive, and distributed information on snow cover in the study area, which could represent a solution to the expensive site access in Antarctica.

2. Study area and methods

2.1. Study area

King George Island (KGI) is located at the northern tip of the Antarctic Peninsula and is the largest of the South Shetland Islands (Fig. 1, S61°50′ to S62°15′ and W57°30′ to W59°01′). The island (surface area of 1310 km^2), which made from volcanic bedrock, lies off in the middle of the South Shetland Islands. Most of the island (approximately 92%) is covered with snow, ice and glaciers and outcrops can be seen only along the shorelines in restricted areas (Lim et al., 2014). The study area is located in the Barton Peninsula of the southwest of KGI, where the King Sejong Station, the first Korean Antarctic Research Station, has been operating since 1988. The Barton Peninsula has a rugged surface topography, with a broad and gentle slope in the central belt, having elevations of 90–180 m above sea level (Lee at al., 2020). Mafic to intermediate lavas are widely distributed in the peninsula, whose eruption history are difficult to determine (Lee et al., 2004). A granodiorite stock with minor fine-grained diorite were produced on the central-northern peninsula, which was intruded during the Eocene (Lee at al., 2020). Much of the bedrock in ice free areas of the peninsula is covered with glacial till. Landscapes changed by periglaciation are prevalent. Soils in King George Island are reported to have formed since the last deglaciation, ca. 9500–6000 years before present (Lopes et al., 2019). Due to the post glacial warming, large glaciated areas became ice free, uncovering glacially striated erratics and bedrock landforms and till deposits, which has the former ice-cap configuration and the glaciation history (Seong et al., 2008).

Since KGI has a cold oceanic climate, weather data for the study area measured at the King Sejong Station during the study year of 2012 show an average annual temperature of –2.5 ± 4.6 °C (1σ), an average relative humidity of 87.1 ± 7.8 %, average precipitation of 598.2 mm, and an average wind speed of 8.1 ± 4.6 m/s, with major wind directions of northwest and southwest. The depth of snow cover ranges from 2–73 cm (Lim et al., 2014), and snow mostly melts in the austral summer. The island is warmer and more humid than other Antarctic regions, with a relatively large water supply from snow melting in the summer (Lee at al., 2020). These characteristics favor periglacial processes and the presence of a generally saturated active layer in summer (Lee et al., 2020); this active layer is up to 1 m depth, and permafrost is present under the active layer (Lee et al., 2004; Lee et al., 2016; Kim et al., 2020). Vegetation is concentrated in abandoned penguin rookeries.

2.2. Collection of GST data

To collect GST data, Maxim iButtons (DS1922L, Hubbart et al., 2005) – instruments consisting of a self-contained temperature sensor and data logger enclosed in a watertight two-terminal stainless-steel can – were placed 2 cm below the ground surface at 131 sites over the Barton Peninsula. Sensors were wrapped in thin plastic to prevent corrosion and were linked with a nylon cord to a nearby marker to aid in finding the sensor after data collection. During the installation of the iButtons, no snow cover was present at any of the sites. The site locations were recorded using GPS and photographs. In order to remove the correlation between observation sites, the iButtons were installed at least 100 m apart. In addition, although the distance between two adjacent points was <100 m, the iButtons were installed if there were distinct ecological, geographical and geological changes. The iButtons were withdrew in the next Antarctic field season, providing a dataset with a length of over one year. Each iButton record has a distinctive identifier and the data loggers are reset. The logging interval was set to 2 h to ensure that the available memory was not overloaded (storage of 4096 readings in memory). The temperature range of the sensor is from –40 °C to 85 °C, in increases of 0.5 °C. The GST data used in this work covered the period from 20 December 2011 to 27 January 2013. Data from three sites were not retrieved because of device errors (total number of applicable sites were 128). Some missing data were obtained with a linear filter for short-term outcomes. Air temperature was measured at the King Sejong Station using an automatic weather station (AWS; Vaisala HMP 45) system.

Due to the low thermal conductivity of snow cover, snow protects the ground from the cold atmosphere during cold period. This effect can be used to reveal snow cover based on GST time series. Danby and Hik (2007) pondered a threshold of 1 °C (4 h sampling rate) to indicate snow-covered ground, and Schmidt et al. (2009) considered a threshold of 0.09 °C (1 h sampling rate). Gądek and Leszkiewicz (2010) and Hrbaacek et al. (2020) assessed the presence of snow cover based on days with GST ≤ 0 °C.

2.3. Statistical approach

First, the GST data were checked for outliers and irregularities; these were corrected where possible or were excluded from the dataset. Then, the variations of the GST data were investigated by multivariate analysis—namely, principal component analysis (PCA), which has been employed for the compression of variables into a set of weighted linear combinations of optimally weighted observed variables, while not losing detail or underlying patterns observed in some or all of the observations sites (Lee et al., 2008; Ko et al., 2010). This method can be used to simplify data, to explore groups in data, and to visualize underlying controls in a multivariate data set. PCA was chosen for this work because an unbiased and effective tool was required that would facilitate the analysis of the hundreds of GST measurements that were made (Winter

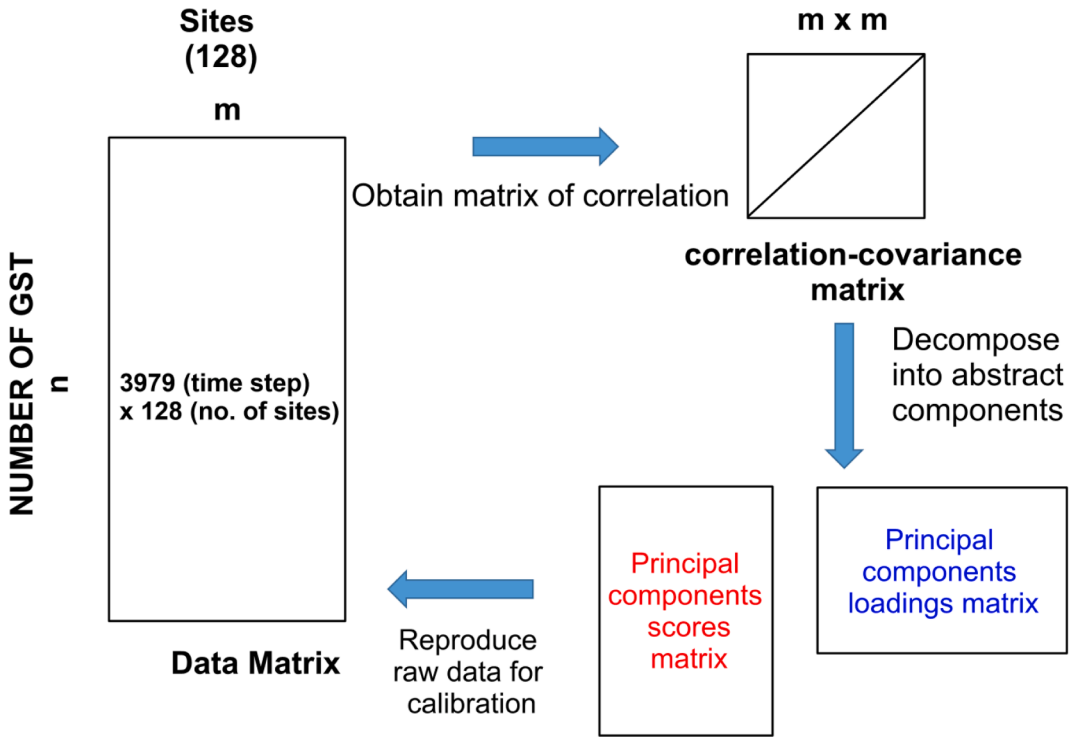

Fig. 2. A schematic diagram showing the basic matrices in the procedure of principal component analysis, modified from Winter et al. (2000).

et al., 2000). PCA recalculates the data in terms of multivariate components that better explain the variation in the data than the original variables. The main reason for using PCA was to identify a few GST patterns that are representative of the general patterns of GST variations over the year 2012 at each site. The PCA procedure is described in numerous statistical textbooks and has been included in most statistical software modules (Winter et al., 2000; Page et al., 2012; Kim and Lee, 2017). Eq. (1) below shows that the PC scores (s) are linear combinations

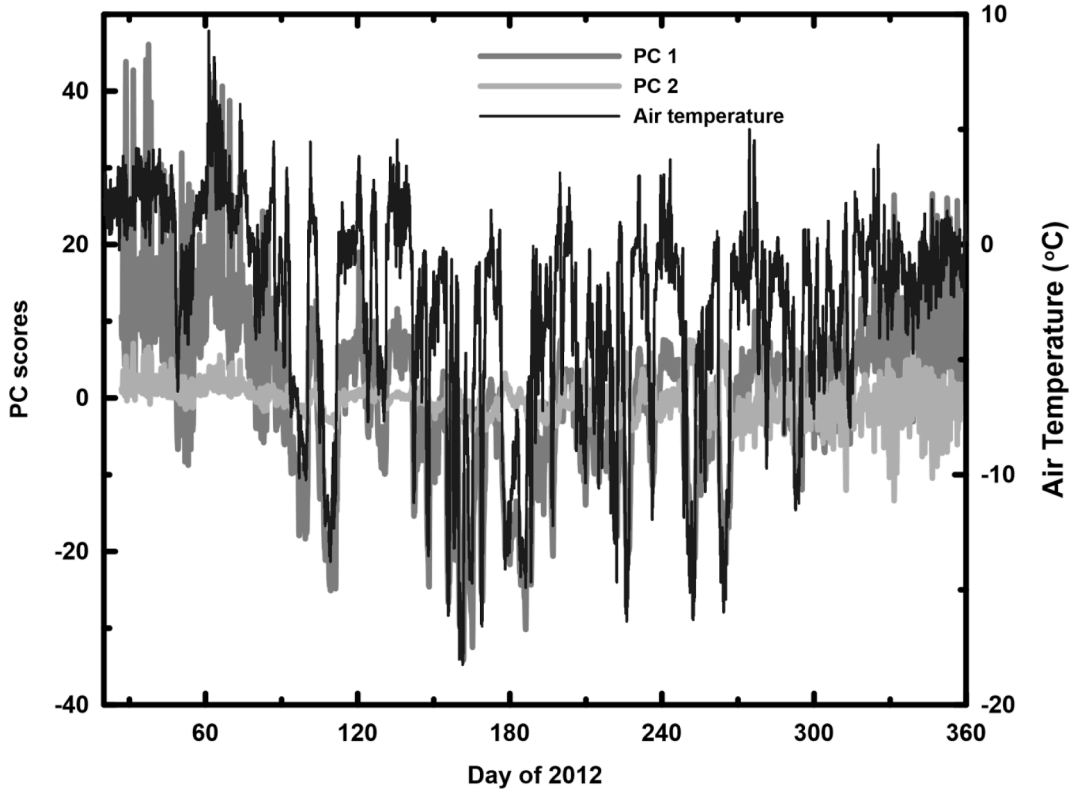

Fig. 3. Time-series of component scores for principal component analysis with air temperature (dark gray for principal component 1, PC 1 and light gray for PC 2). PC1 and air temperatures show similar patterns.

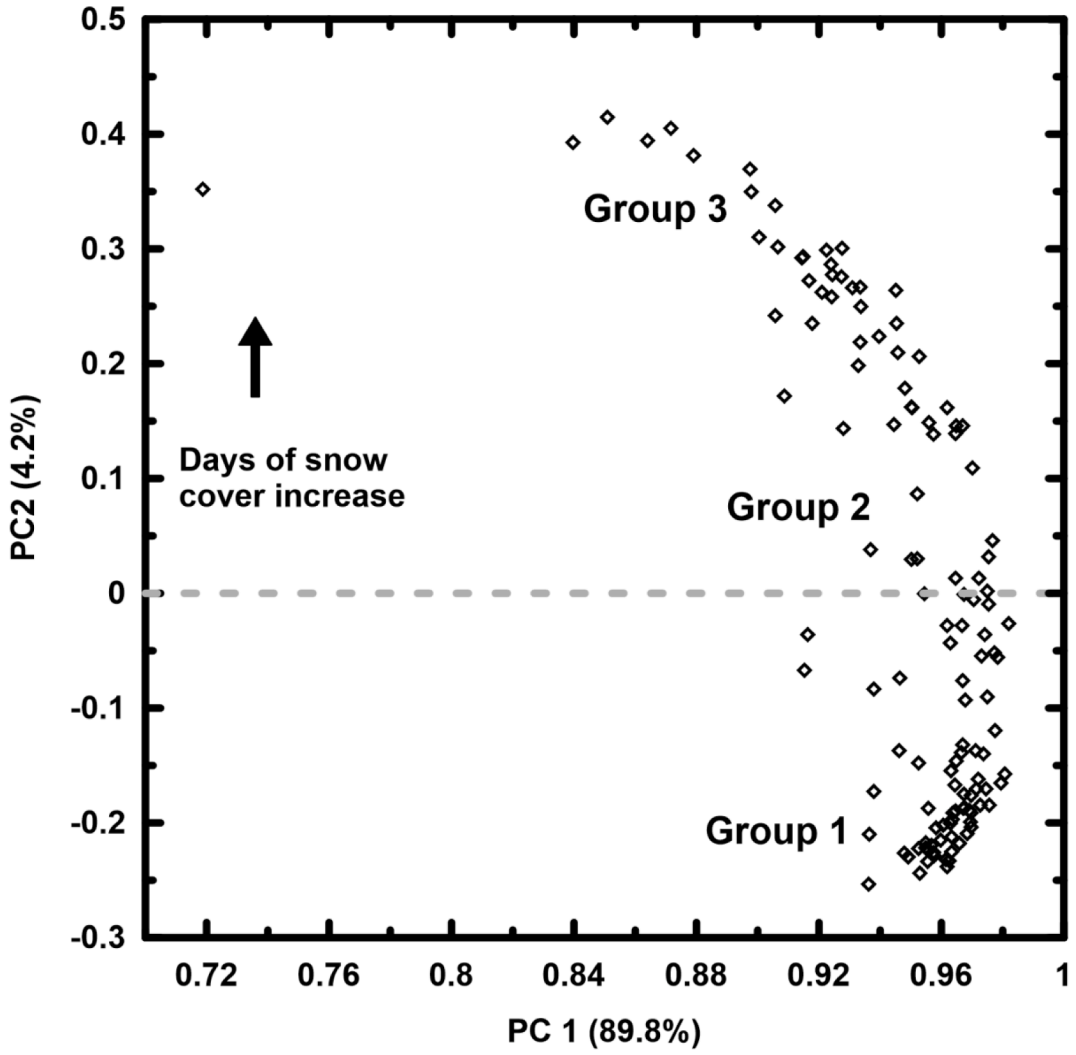

Fig. 4. A scatter plot of component loadings between PC1 and PC2 for GST in the Barton Peninsula. The point in the left side of the diagram is an outlier.

of the standardized data (x) with the loadings (l) as the coefficients: (O'Rourke and Hatcher, 2013):

$$s_{n,c} = \sum x_{n,e} \times l_{e,c} \quad (1)$$

where n identifies the GST, e is the site information, and c identifies the principal component (O'Rourke and Hatcher, 2013; see the schematic diagram in Fig. 2).

In this study, the principal components of an n-column, m-row array was computed using the IDL (Interactive Data Language) PCOMP function where n is the number of independent variables (the number of measurements with temporal resolution) and m is the number of observations or samples (Lee et al., 2008; Kim and Lee, 2017; see Fig. 2). If the variables of the PCA are measured in large variations in magnitude, it is a good way to choose the sample correlation coefficient matrix to compute the principal components instead of covariance coefficient matrix (Lee et al., 2008). In the correlation matrix, each variable is normalized to unit variance so that they contribute equally (Ko et al., 2010). Identification of systematic patterns of both temporal and spatial variabilities in the original GST matrix is attained by calculation of the component loadings and scores that reflect the underlying correlation structure of the dataset (Kim and Lee, 2017).

3. Results and discussion

To relate the GST to geographical factors, such as latitude, longitude, elevation, slope or aspect of the site and proximity to the ocean, the mean values of the seasonal GST were plotted with an image taken by KOMPSAT-2 (KOrea Multi-Purpose Satellite) on 16 January 2013 (Fig. 1). Fig. 1 illustrates (a) the mean GST values for JJA, (b) the mean GST values for DJF, (c) the difference between the mean GST values for JJA and those for DJF, and (d) the mean GST values for the whole observations period. As shown in Fig. 1, no geographical or physical factors were not significantly related to the GST. We excluded the relationship between the GST and slope and aspect of the site because it was difficult to quantify the effect of slope or aspect of the site (Dahlke and Lyon, 2013). Therefore, to search for other factors that can be related to the GST, we applied PCA to the GST dataset.

3.1. Principal component analysis

PCA can be useful for understanding the responses of the GST to air temperature with the presence or absence of snow cover. By determining the extent to which the GST variations at individual sites relate to the statistically computed GST variations, the areal distribution of GST patterns was mapped throughout the study area. It is expected that this information will be beneficial for understanding the response of the GST system to natural processes, such as fluctuations of air temperature, in

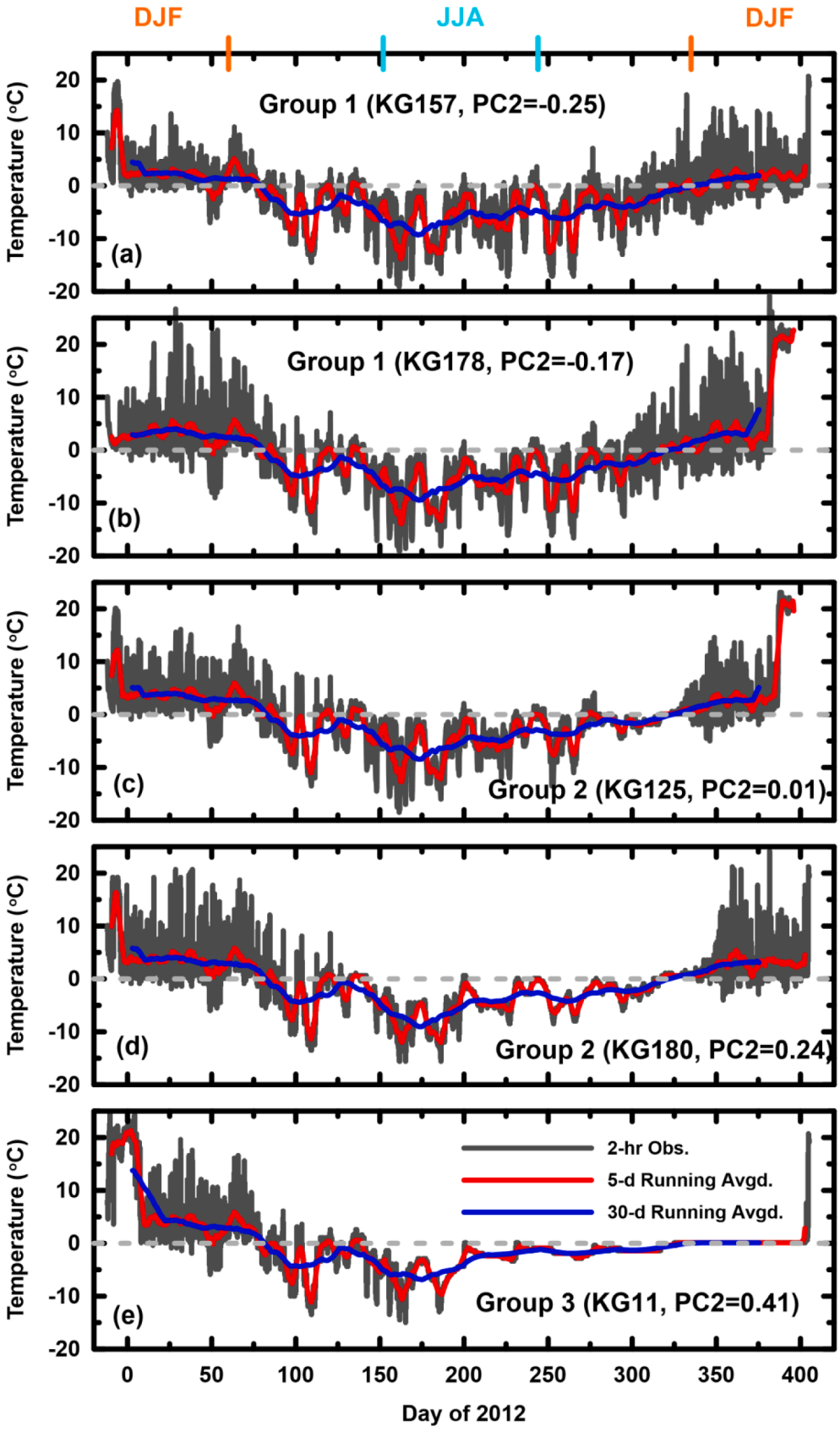

Fig. 5. Time-series of observed GST by groups separated using PCA. Five and thirty day averaged data were also presented. (a) KG157, (b) KG178, (c) KG125 (d) KG180 and (e) KG11. Note that the distance between KG 178 and KG 180 is about 150 m away.

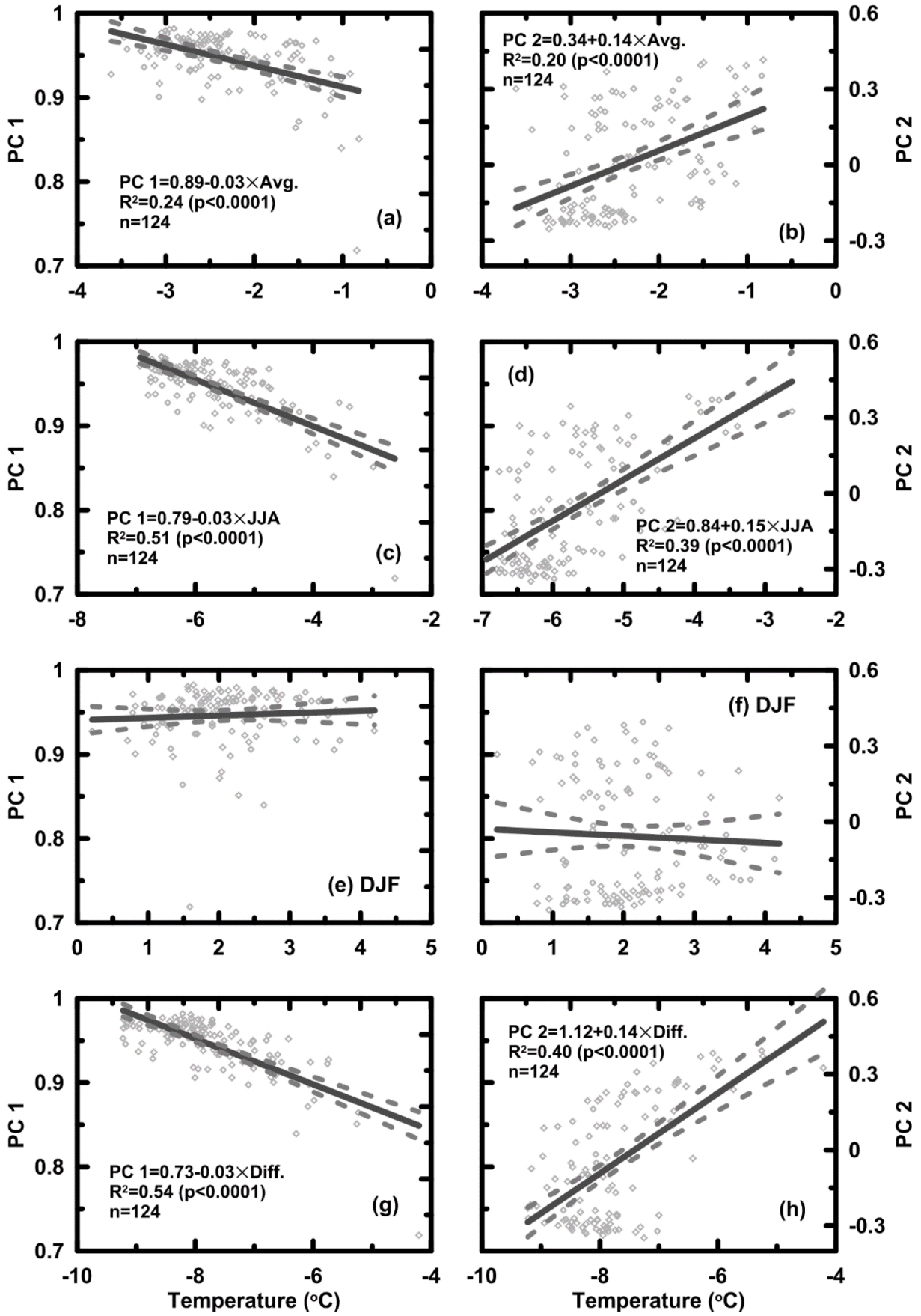

Fig. 6. Statistical relationships between mean values of seasonal GST and principal components (PCs). GST observed during JJA are correlated with both PC1 and 2.

addition to distinguishing the presence or absence of snow cover. One advantage of this type of information is that it enables the selection of a subset of only a few index sites that could be measured instead of the entire set with little loss of information (Winter et al., 2000).

It came to know that the first principal component (PC1) accounted for 89.8% of the variance in the GST data, and the second principal component (PC2) accounted for 4.2% of the variance (i.e., PC1 + PC2 = 94% of the total variance). Fig. 3 shows a GST time series of component scores, which graphically represents the variance in the two-hour data, together with air temperature. Component scores are a measure of the temporal resemblance between the observed pattern of the GST for a given time and each principal component. The PC1 decreased during the first half of the study period and then increased during the rest of the study period, whereas PC2 did not show any significant trend. The pattern of air temperature is closely related to the GST time-series for PC1.

The first two components were selected because this study seeks to identify the main patterns driving temperature variations. A bivariate plot of the scores of the selected PC provides more information than any scatter plot from the original variables. In general, the first few PCs are sensitive to outliers that inflate variance or distort covariance (Rencher, 1995). We used bivariate plots of the first two PCs to search for outliers that could exert undue influence. The results for KG100 lie in the upper-left corner of the plot (Fig. 4). The GST from the KG100 showed fluctuations; however, there were no fluctuations after day 94, which can be explained by the presence of snow cover after this date. This outlier was excluded from further study.

In Fig. 4, the first principal component is plotted along the horizontal axis and PC2 is plotted along the vertical axis. The PCA results can be divided into three groups based on the loading values of PCs 1 and 2 to identify the main factor affecting the GST variations in each group. GSTs that had lower loadings on PC1 and higher loadings on PC2 (upper-middle of the diagram) were designated as Group 1 (Fig. 4). At the other extreme, GSTs that had higher loadings on PC1 and lower loadings on PC2 in (upper-right side of the diagram) were designated as Group 3. Interestingly, PC2 explained 4.2% of the total variation, but it plays a significant role to determine the separation of the group (PC1 also varies). To explore the factor that most influenced the GST in each group and how the GST was influenced by the factor, we selected three observations with the highest loading value for PCs 1 and 2 after principal component analysis with two middle PCs 2 values (KG 178 and KG 180 for Fig. 5b and d, respectively). The distance between two sites of KG178 and K180 is approximately 150 m away. The loading value is a dimensionless score of how much each observation point represents the GST variations—that is, an observation point with a high loading value better represents the GST variations. In this study, KG157, KG125, and KG11 were selected as representative of groups 1, 2, and 3, respectively (Fig. 5a, c and e). The GST pattern of each group, illustrated in Fig. 5, can be explained by the presence of snow cover. The definition of "*presence of snow cover*" in this work means snow cover to the extent that it may be present but does not affect the GST patterns. Based on the PCA results, the three groups can be explained as follows: Group 1: absent snow cover throughout the whole study period; Group 2: intermittent snow cover; and Group 3: present snow cover during JJA and lasted through the rest of the study period. In the next section, we will discuss the absence/presence of snow cover.

3.2. Effect of snow cover on GST

The presence of snow cover greatly affects GST and ground heat fluxes because the thermal conductivity of snow (0.1 to 0.5 W m^{-1} K^{-1}) is much lower than that of mineral soils (Zhang, 2005). GST measurements, in particular using iButtons, provide a powerful and relatively inexpensive method to track the distribution of snow cover (Lundquist and Lott, 2008). Spatio-temporal variations of GST in the Barton Peninsula, Antarctica, reflect a variability of surface energy fluxes and

Table 1
Statistics of representative site of each group.

Period	Site		
	Group 1 (KG157, °C)	Group 2 (KG125, °C)	Group 3 (KG11, °C)
Whole study period	–1.96 ± 5.7	–0.58 ± 5.9	–0.05 ± 5.8
JJA*	–5.32 ± 4.6	–4.55 ± 3.7	–3.09 ± 2.6
DJF*	2.05 ± 4.2 (2.64 ± 4.4, 1.31 ± 3.7)	4.23 ± 5.6 (3.86 ± 4.4, 4.70 ± 6.9)	4.29 ± 6.9 (7.6 ± 7.8, 0.10 ± 0.0)

* JJA and DJF denote July, June and August and December, January and February, respectively. Values of parenthesis in DJF represents 2nd period of DJF during the study period.

are mostly related to the variability of climatic, topographic conditions, and material differentiate on the surface. In extreme environments such as Antarctica, the beginning of snowmelt can be recognized by the time when the GST rises to 0 °C and remains the same for several days. Thus, GST provides not only an indication of soil temperature and the extent of ground freezing, but, when measurements are sufficiently distributed, also provides spatial representations in the presence or absence of snow cover.

In Fig. 5, three distinct GST patterns were extracted using PCA, and the patterns indicate the presence/absence of snow cover. Although the two sites (KG178 and KG180) were close, the patterns of two sites are different because of local properties. From Fig. 5a and 5c, it is evident that the GST for Group 1 indicates the absence of snow cover during the whole study period (strong diel variation of GST), whereas the GST for Group 3 suggests the presence of snow cover during JJA and lasted for the rest of the study period. The GST pattern of Group 2 implies that snow cover was present until the beginning of the second DJF of the study period, but also suggests that the snow cover was not as thick as in Group 3. Based on the three approaches described in the method section, for example, the site (PC 2, KG125) had snow cover for nine days (days 317–326), and the melt-out date (i.e., the time when the snow cover is depleted and no further release of meltwater occurs, which allows the ground surface to warm above 0 °C) is day 326 (Schmid et al. 2012).

Fig. 6 allows the seasonal mean GST to be related to both air temperature and snow cover. As we found in the previous section, principal component (PC) 1 is associated with air temperature and PC 2 is linked with the presence/absence of snow cover. Both PCs show a good correlation with the mean GST of JJA. Principal component 1 is negatively correlated with that of JJA, whereas PC2 is positively correlated with that of JJA. As the value of PC1 increases, the GST pattern becomes more similar to the air temperature pattern. If the GST of a site is directly influenced by air temperature during the austral winter, the GST of the site can be more variable and lower than at other sites. Similarly, as the value of PC2 increases, the GST pattern is affected by the presence of snow cover; due to the presence of snow cover, the GST of a site will not change significantly, with the GST being dependent upon the duration and/or depth of snow cover.

Comparing the temporal variability of the GST among each group may allow the effect of snow cover on GST in this region to be characterized. Over the whole study period, the mean GST of Group 1 (KG157) and Group 2 (KG125) are lower than that of Group 3 (KG11, $p < 0.001$, see Table 1). During JJA, the mean GST of groups 1 and 2 are also lower than that of Group 3 ($p < 0.001$). However, during DJF, the mean GST of Group 1 is lower than those of groups 2 and 3 ($p < 0.001$), although the mean GST of Group 2 is not statistically significantly lower than that of Group 3. In this study, since the GST was observed between December 2011 and January 2013, there were two DJF periods. As the iButtons were installed in snow-free areas, at all observation sites, the GST patterns in the first DJF were similar to the air temperature patterns. However, in the second DJF, the GST patterns were modified by the absence/presence of snow cover. At all three sites, the mean values of GST were different between the two DJF periods ($p < 0.005$, Table 1).

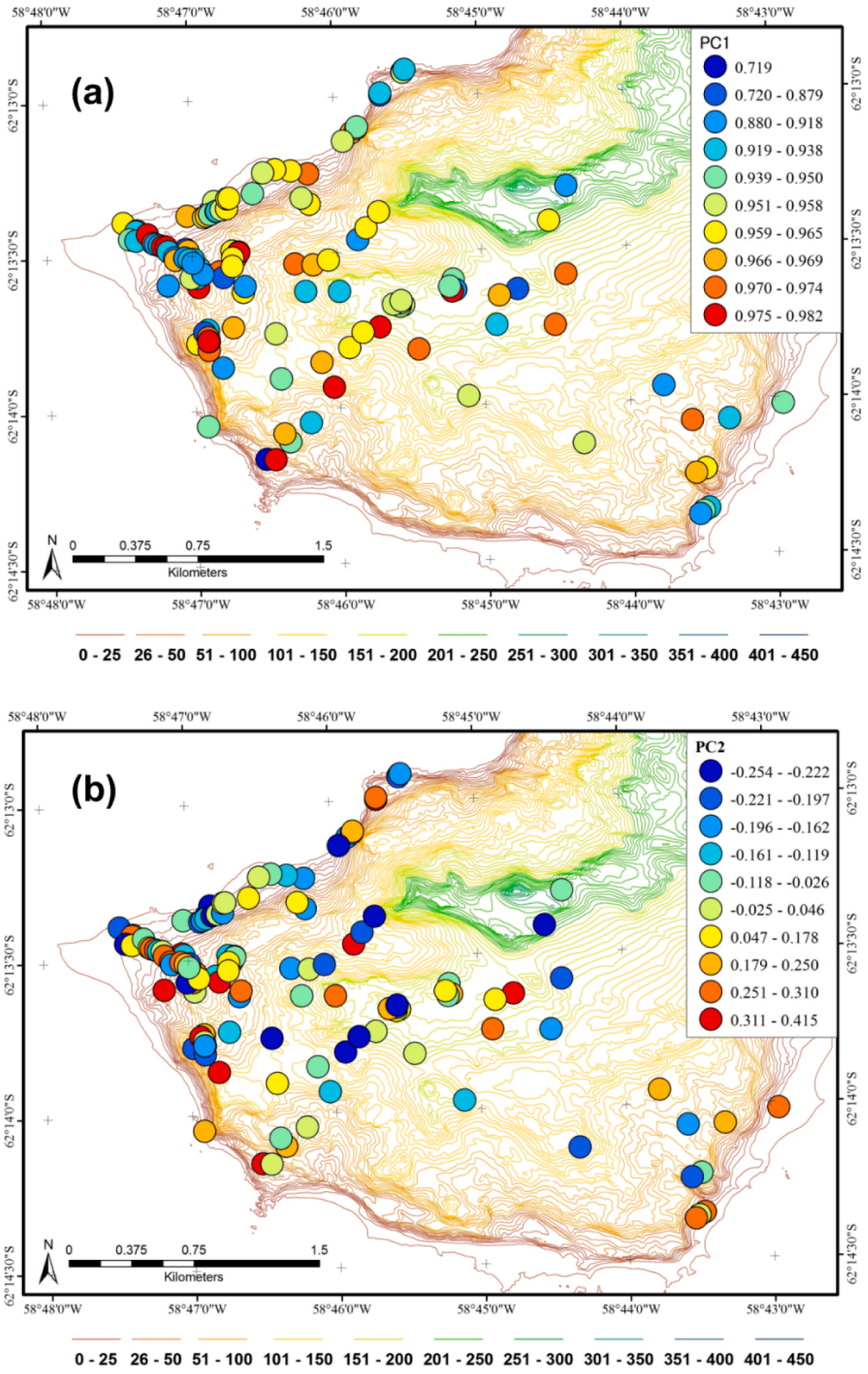

Fig. 7. The spatial variations of the component loadings of PC1 (a) and PC2 (b) over the Barton Peninsula. The contours represent elevations from the digital topography map (1:5000).

Due to the presence of snow cover in the second DJF, the mean DJF GST of Group 3 changed dramatically 7.6 to 0.1 °C. However, due to the insulating effect of intermittent snow cover, the mean DJF GST of Group 2 increased 3.9 to 4.7 °C ($p < 0.005$).

Snow cover plays an important to role in water supply from snow melting in polar regions, and especially in Antarctica. Snow cover can be used as a proxy for water supply during the austral summer. Mosses are a dominant terrestrial plant in Antarctica, in particular on the western Antarctic Peninsula, where they are the predominant land cover (Prather et al., 2019). Mosses are poikilohydric organisms that rely directly on the environment for water and lack mechanisms to prevent desiccation, making them sensitive to changes in precipitation regimes

at both the micro- and macro-levels (Kennedy, 1993). Therefore, it can be assumed that the abundance and productivity of mosses in the study area will be influenced by precipitation. A map of the areal distribution of the GST, illustrated in Fig. 7, can be used to correlate with the distribution of mosses in the study area. We suggest that high loading values of PC1 represent the absence of snow cover (Group 1), whereas high loading values of PC2 represent the presence of snow cover (Group 3). In this sense, Group 2 affected by the intermittent snow cover would explain distribution of mosses if a map of the moss distribution can be generated (Shin et al., 2014).

4. Conclusions

In polar environments, and especially in Antarctica, snow cover plays an important role in water supply from snow melting. Although the cost of site access is high in Antarctica, GST measurements using iButtons is a powerful and relatively inexpensive tool to track the distribution of soil temperature and snow cover (Lundquist and Lott, 2008). In this study, annual variations of GST on King George Island, at the margin of maritime Antarctica, were observed at 128 sites between December 2011 and January 2013. The iButtons were installed in snow-free areas. Observations of GST can provide spatial information about the absence/presence of snow cover, which is very difficult to obtain. Principal component analysis was used to separate the 128 GST data into three groups: absent snow cover (Group 1), intermittent snow cover (Group 2), and present snow cover (Group 3). Principal components 1 and 2 are associated with air temperature and snow cover, respectively. Snow cover can supply water to the ecosystem, and the GST pattern of Group 2 may imply to abundance and productivity of mosses in the study area. Using approaches suggested by previous studies, snow cover showed up nine days (day of 317 and 326), and the melt-out date was found to be day 326. We believe that the GST data and statistical approaches utilized in this study can be useful in other maritime Antarctic studies.

Declaration of Competing Interest

The authors declare that they have no known competing financial interests or personal relationships that could have appeared to influence the work reported in this paper.

Acknowledgments

This work was financially supported by research grant (PE21130) from the Korea Polar Research Institute. This work was partially supported by the National Research Council of Science & Technology (NST) grant of the Korea government (MSIP) (CAP-17-05-KIGAM) and KIMST20190361 from the Korea Ministry of Oceans and Fisheries. We appreciate two anonymous reviewers, whose comments led to significant improvements.

References

Beltrami, H., 1996. Active Layer Distortion of Annual Air/Soil Thermal Orbits. Permafrost Periglac. Process. 7 (2), 101–110.
Bender, E., Lehning, M., Fiddes, J., 2020. Changes in Climatology, Snow Cover, and Ground Temperatures at High Alpine Locations. Front. Earth Sci. 8, 100.
Cannone, N., Guglielmin, M., 2009. Influence of vegetation on the ground regime in continental Antarctica. Geoderma 151, 215–223.
Convey, P., Peck, L.S., 2019. Antarctic environmental change and biological responses. Science. Advances 5 (11), eaaz0888.
Danby, R.K., Hik, D.S., 2007. Variability, contingency and rapid change in recent subarctic alpine tree line dynamics. J. Ecol. 95, 352–363.
Dahlke, H.E., Lyon, S.W., 2013. Early melt season snowpack isotopic evolution in the Tarfala valley, northern Sweden. Ann. Glaciol. 54 https://doi.org/10.3189/2013AoG62A232.
de Pablo, M.A., Ramos, M., Molina, A., 2017. Snow cover evolution, on 2009–2014, at the Limnopolar lake CALM-S site on Byers Peninsula, Livingston Island, Antarctica. Catena 149, 538–547.
Gądek, B., Leszkiewicz, J., 2010. Influence of snow cover on ground surface temperature in the zone of sporadic permafrost, Tatra Mountains, Poland and Slovakia. Cold Reg. Sci. Technol. 60 (3), 205–211.
Guglielmin, M., 2006. Ground surface temperature (GST), active layer and permafrost monitoring in continental Antarctica. Permafrost Periglac. Process. 17 (2), 133–143.
Guglielmin, M., Worland, M.R., Cannone, N., 2012. Spatial and temporal variability of ground surface temperature and active layer thickness at the margin of maritime Antarctica, Signy Island. Geomorphology 155–156, 20–33.
Hrbacek, F., Cannone, N., Knazkova, M., Malfasi, F., Convey, P., Guglielmin, M., 2020. Effect of climate and moss vegetation on ground surface temperature and the active layer among different biogeographical regions in Antarctica. Catena 190, 104562.
Hubbart, J., Link, T., Campbell, C., Cobos, D., 2005. Evaluation of a low-cost temperature measurement system for environmental applications. Hydrol. Process. 19 (7), 1517–1523.
Kennedy, A.D., 1993. Water as a Limiting Factor in the Antarctic Terrestrial Environment: A Biogeographical Synthesis. Arct. Alp. Res. 25 (4), 308–315.
Kim, J., Jeen, S.-W., Lim, H.S., Lee, J., Kim, O.-S., Lee, H., Hong, S.G., 2020. Hydrogeological characteristics of groundwater and surface water associated with two small lake systems on King George Island. J. Hydrol. 590, 125537.
Kim, J.M., Lee, J., 2017. Time-series for evaluating hydrological responses of pore-water pressure to rainfall in a slope. Hydrol. Sci. J. 62, 1412–1421.
Ko, K.-S., Lee, J., Lee, K.-K., Chang, H.-W., 2010. Multivariate statistical analysis for groundwater mixing ratios around underground storage caverns in Korea. Carbonates Evaporites 25, 35–42.
Lee, J., Ko, K.-K., Kim, J.-M., Chang, H.-W., 2008. Multivariate statistical analysis of underground gas storage caverns on groundwater chemistry in Korea. Hydrol. Process. 22, 3410–3417.
Lee, J., Hur, S.D., Lim, S.H., Jung, H., 2020. Isotopic characteristics of snow and its meltwater over the Barton Peninsula. Antarctica. Cold Regions Science and Technology 173.
Lee, J.Y., Lim, H.S., Yoon, H.I., 2016. Thermal characteristics of soil and water during summer at King Sejong Station, King George Island, Antarctica. Geosci. J. 20, 503–516.
Lee, Y.I., Lim, H.S., Yoon, H.I., 2004. Geochemistry of soils of King George Island, South Shetland Islands, West Antarctica: Implications for pedogenesis in cold polar regions. Geochim. Cosmochim. Acta 68, 4319–4333.
Lim, H.S., Park, Y., Lee, J.-Y., Yoon, H.I., 2014. Geochemical characteristics of meltwater and pondwater on Barton and Weaver Peninsulas of King George Island, West Antarctica. Geochem. J. 48, 409–422.
Lopes, D., Schaefer, C., Souza, J., Oliveira, F., Simas, F., Daher, M., Gjorup, D., 2019. Concretionary horizons, unusual pedogenetic processes and features of sulfate affected soils from Antarctica. Geoderma 347, 13–24.
Lundquist, J.D., Lott, F., 2008. Using inexpensive temperature sensors to monitor the duration and heterogeneity of snow-covered areas. Water Resour. Res. 44 (4), W00D16.
Luo, D., Jin, H., Bense, V.F., 2019. Ground surface temperature and the detection of permafrost in the rugged topography on NE Qinghai-Tibet Plateau. Geoderman 333, 57–68.
Nyamgerel, Y., Han, Y., Kim, S., Hong, S., Lee, J., Hur, S., 2020. Chronological characteristics for snow accumulation on Styx Glacier in northern Victoria Land. Antarctica. Journal of Glaciology 66 (260), 916–926.
Obu, J., Westermann, S., Vieira, G., Abramov, A., Balks, M.R., Bartsch, A., Hrbacek, F., Kaab, A., Ramos, M., 2020. Pan-Antarctic map of near-surface permafrost temperatures at 1km2 scale. The Cryosphere 14, 497–519.
Oliva, M., Hrbacek, F., Ruiz-Fernandez, J., de Pablo, M.A., Vieira, G., Ramos, M., Antoniades, D., 2017. Active layer dynamics in three topographically distinct lake catchments in Byers Peninsula (Livingston Island, Antarctica). Catena 149, 548–559.
O'Rourke, N., Hatcher, L., 2013. A Step-by-Step Approach to Using SAS for Factor Analysis and Structural Equation Modeling, 2nd Ed. SAS Institute Inc., Cary, NC.
Page, R.M., Lischeid, G., Epting, J., Huggenberger, P., 2012. Principal component analysis of time series for identifying indicator variables for riverine groundwater extraction management. J. Hydrol. 432–433, 137–144.
Pedersen, S.H., Tamstorf, M.P., Abermann, J., Westergaard-Nielsen, A., Lund, M., Skov, K., Sigsgaard, C., Mylius, M.R., Hansen, B.U., Liston, G.E., Schmidt, N.M., 2018. Spatiotemporal Characteristics of Seasonal Snow Cover in Northeast Greenland from in Situ Observations. Arct. Antarct. Alp. Res. 48 (4), 653–671.
Prather, H.M., Casanova-Katny, A., Clements, A.F., Chmielewski, M.W., Balkan, M.A., Shortlidge, E.E., Rosenstiel, T.N., Eppley, S.M., 2019. Species-specific effects of passive warming in an Antarctic moss system. R. Soc. open sci. 6, 190744.
Rencher, A.C., 1995. Methods of Multivariate Analysis. John Wiley & Sons Inc, New York.
Schmid, M.O., Gubler, S., Fiddes, J., Gruber, S., 2012. Inferring snowpack ripening and melt-out from distributed measurements of near-surface ground temperatures. The Cryosphere 6 (5), 1127–1139.
Shin, J.-I., Kim, H.-C., Kim, S.-I., Hong, S.G., 2014. Vegetation abundance on the Barton Peninsula, Antarctica: estimation from high-resolution satellite images. Polar Biol. 37 (11), 1579–1588.
Staub, B., Delaloye, R., 2017. Using Near-Surface Ground Temperature Data to Derive Snow Insulation and Melt Indices for Mountain Permafrost Applications. Permafrost Periglac. Process. 28 (1), 237–248.
Teubner, I.E., Haimberger, L., Hantel, M., 2015. Estimating Snow Cover Duration from Ground Temperature. Journal of Applied Meteorology and Climatology 54 (5), 959–965.
Vieira, G., Mora, C., Faleh, A., 2017. New observations indicate the possible presence of permafrost in North Africa (Djebel Toubkal, High Atlas, Morocco). The Cryosphere 11 (4), 1691–1705.

Winter, T.C., Mallory, S.E., Allen, T.R., Rosenberry, D.O., 2000. The use of principal component analysis for interpreting ground water hydrographs. Ground Water 38, 234–246.
Zhang, T., 2005. Influence of the seasonal snow cover on the ground thermal regime: An overview. Rev. Geophys. 43, RG4002.
Zhao, J.-Y., Chen, J., Wu, Q.-B., Hou, X., 2018. Snow cover influences the thermal regime of active layer in Urumqi River Source, Tianshan Mountains. China. Journal of Mountain Science 15 (12), 2622–2636.